Viscoelasticity of Monodisperse Comb Polymer Melts

ARTICLE *in* MACROMOLECULES · MAY 2006

Impact Factor: 5.8 · DOI: 10.1021/ma060018f

5 AUTHORS, INCLUDING:

Nathanael Inkson
CD-adapco
8 PUBLICATIONS **408** CITATIONS
SEE PROFILE

Tom C B Mcleish
Durham University
227 PUBLICATIONS **8,294** CITATIONS
SEE PROFILE

Christine M. Fernyhough
The University of Sheffield
30 PUBLICATIONS **825** CITATIONS
SEE PROFILE

Viscoelasticity of Monodisperse Comb Polymer Melts

N. J. Inkson,*,† R. S. Graham,‡ T. C. B. McLeish,‡ D. J. Groves,‡ and C. M. Fernyhough§

School of Applied Mathematics, University of Leeds, Leeds, LS2 9JT, United Kingdom; Interdisciplinary Research Centre in Polymer Science and Technology, School of Physics and Astronomy, The University of Leeds, Leeds, LS2 9JT, United Kingdom; and Department of Chemistry, University of Sheffield, Sheffield S3 7HF, UK

Received January 4, 2006; Revised Manuscript Received April 5, 2006

ABSTRACT: The experimentally determined zero-shear viscosity of entangled branched polymers shows dramatic variation due to the topological arrangements of the branches in branched polymer melts. The position of the branch points, the arm length, and number of the arms are essential to defining the rheological behavior. Recent advances in molecular tube models have led to a much greater understanding of the linear rheology of linear, star, H-shaped, pom-pom, and comb polymers. We correct and extend existing molecular theories for the linear viscoelasticity of comb polymer melts, especially in accounting for (1) polydispersity and (2) the path length of backbone extremities. We compare the predictions with linear rheological data of nearly monodisperse polybutadiene combs. We then predict the zero-shear viscosity for monodisperse comb polyethylenes with varying arm lengths, backbone lengths, and number of arms. For a fixed molecular weight, we find that combs with the longest arms but few branch points give the highest predicted zero-shear viscosities and that they obey an exponential dependence on the length of the arms in the same way as star polymers. We find that combs with short arms, under four entanglements, lie below the 3.4 power law obeyed by linear polymers. All other comb topologies are bounded by these extremes.

I. Introduction

Advances in the tube theory[1,2] have allowed the creation of detailed models for monodisperse branched polymers that describe the linear rheology of these melts. The only parameters used by these models are determined by the chemistry of the polymer chain and are M_e, the entanglement molecular weight, and τ_e, the relaxation time of an entanglement segment at a given temperature. Structural variables that define the topology of the branched structure also define the model, i.e., the backbone length, the number of arms, and the length of them. Essential to this program has been the availability of monodisperse, controlled architecture polymers, usually made by anionic polymerization.[3] Of special interest is the "comb" architecture.[4] This molecule shares some dynamical features of linear melts (associated with the backbone) and those of star polymers (associated with the arms).

We explore how the zero-shear viscosity varies for monodisperse comb polymers with varying arm lengths, backbone lengths, and number of arms. We also predict rheology of very highly branched combs. The comb model in the linear rheological regime builds upon the Milner−McLeish model of star polymers[5] for the arm relaxation dynamics along with the effect of dynamic dilution of the remaining network of material. The time for the arms to reach the branch point then sets the time scale of the relaxation of the first segments of the backbone. The backbone initially relaxes in a fashion similar to a star arm, by fluctuation at the ends but with drag set by the arms and concentrated at the branch points. However, at some distance along the backbone from the free ends, the fluctuation relaxation time of the backbone becomes longer than the reptation time of the backbone, and the rest of the polymer relaxes by reptation. Note that this reptation time is much longer than that of a linear polymer due to the large effective friction from the arms. This, in turn, is very sensitive to the length of the entangled arms because the arm relaxation process, which allows branch point diffusion, depends exponentially on the arm length.

II. Experimental Section

Synthesis and Rheology. The polybutadiene comb synthesis has previously been reported in detail in the literature.[4,6] Here we shall briefly summarize the rheological experiments. The polymer samples were vacuum-dried, compacted using a piston and cylinder, and then premolded to a suitable thickness and geometry using a template and platen press. The press molding temperature was performed typically at 90 °C under a vacuum or nitrogen atmosphere to prevent oxidation. All shear rheology measurements were made using Rheometrics ARES or RDAII rotational rheometers under a nitrogen atmosphere. The linear relaxation spectrum, $G'(\omega)$ and $G''(\omega)$, was measured using a geometry of either 10 mm diameter parallel plates or a 10 mm diameter cone and plate with 2° included angle. Time−temperature superposition of the frequency sweep data was used to obtain master curves from measurements made between −80 and 60 °C.

III. Theory

The model used in this paper follows largely the same comb theory as outlined in ref 6. However, there are some differences in the resulting mathematical expressions used here, which arise from both corrections to former errors and developments in the physics. These differences are summarized in Table 1. A variant of this comb model has been recently published to analyze the original rheological study of combs by Kapnistos et al.[22] However, their model is different than ours in its treatment of polydispersity (a simple weighted average), choice of the dilution exponent, and the prefactors for the early relaxation times for the comb backbones.

In the following we improve the quantitative accuracy of the tube model for entangled combs by extending the model in two

† School of Applied Mathematics, University of Leeds.
‡ School of Physics and Astronomy, University of Leeds.
§ University of Sheffield.

10.1021/ma060018f CCC: $33.50
Published on Web 05/20/2006 PAGE EST: 10.8

Table 1. Corrected Equations in This Paper Compared to Ref 6

equation for relaxation times	equation in ref 6	equation in this paper	explanation
early arm	3	4	no change
late arm	5	5	the factor 2 should be in the numerator not the denominator within the square root (see Appendix A)
early light comb backbone	12	8	no change
late time comb backbone	10	10	the factor 2 should be in the numerator not the denominator within the square root (see Appendix A)
light comb reptation	13	12	prefactor should be 25/8 (see text for derivation)
early highly branched comb backbone	15	9	prefactor is smaller by factor 2 (see Appendix B)
highly branched comb reptation	16	12	there is only one equation for backbone reptation

significant ways: (1) by accounting for polydispersity in the arm molecular weight and (2) by calculating the influence on the branch point motion of the position of the final grafted arm along the backbone. The general procedure for calculating the small-angle oscillatory shear modulus starts by computing the arm relaxation spectrum via the tube dilation model for arm retraction. The time scale of the arm relaxation up to the branch point then enables a calculation of backbone relaxation times. Numerical integration over the length of the arms and backbones then provides the storage and loss modulii.

In recent literature, there has been some uncertainty in the validity of the dynamic dilution process[7,8] used in this approach. However, more detailed constraint-release models of entangled star arms show that the single-mode dynamic tube dilution (DTD) picture is valid as an approximation for linear rheological prediction[9] so we use this model for simplicity. The polymers modeled are highly entangled. We define the dimensionless number of entanglements as $s_a = M_a/M_e$ for the number of arm entanglements. The number of backbone entanglements, s_b, is defined similarly. M_a and M_b are the molecular weights of the arms and backbones, respectively. τ_e is the Rouse relaxation time of one segment of the entanglement molecular weight. The value of τ_e is also temperature dependent.

To account for the modulus reduction by effective dilution with successive removal of entanglements, we also require the dependence of plateau modulus on concentration of entangled chains Φ, $G(t) \sim \Phi^{\alpha}$. We choose the value of the dilution exponent, $\alpha = {}^4/_3$, for Θ or melt conditions. The effective modulus of an entanglement network is a function of the fraction of material that acts as solvent on a given time scale. For more information about the dynamic tube dilution theory (DTD) see refs 5 and 10. The fraction of polymer chain that can confine a given section of a molecule is related to the distance away from the free end. The general formula for the linear relaxation modulus is given by[6]

$$G(t) = \int_0^1 \frac{\partial G(\Phi(x))}{\partial x} e^{-t/\tau}(x)\, dx \qquad (1)$$

where $\Phi(x)$ is the fraction of unrelaxed chain and x is the normalized distance along the chain. $\tau(x)$ is the mean waiting time for a free end to visit the tube segment at tube coordinate x. In the case of H-polymers, pom-poms, combs, and molecular brushes we can divide the chain into arm and backbone coordinates separately and write eq 1 as

$$G(t) = G_0(\alpha+1)\left(\int_0^1 \phi_b^{\alpha+1}(1-x_b)^{\alpha} e^{-t/\tau_b(x_b)}\, dx_b + \int_0^1 (1-\phi_a x_a)^{\alpha}\phi_a e^{-t/\tau_a(x_a)}\, dx_a\right) \qquad (2)$$

where ϕ_a and ϕ_b are the arm and backbone volume fractions and x_a and x_b are the dimensionless coordinates along the arm and the backbone, respectively.

Figure 1 shows the dimensionless coordinates used to describe a comb molecule. The arm coordinate, x_a, runs from zero at the free end to one at the branch point. To compute the backbone length and volume fraction, we count all material between the two outermost attachment points as backbone. Since we take the branch points to be evenly spaced, the dimensionless backbone length is given by $s_b = (M_b - 2/(q+1))/M_e$. Thus, the backbone coordinate, x_b, runs from one at the center of the backbone to zero at the final branch point. In the derivation presented in the main section of this paper we further assume that all arms have the same length, that of the grafted arms, to follow the approach of ref 6. This ignores the possibility that one of the arms on the end branch points may be longer or shorter depending on the backbone length and position of the grafted arms. To correct this simplification, we have performed a detailed calculation of the simultaneous relaxation of two different length comb arms within the dynamic dilution framework. Details of these calculations are contained in Appendix C. Our results indicate that, for the combs in this study, the influence of this correction is relatively small, but for completeness, we include this correction whenever we compare directly to experimental data. To allow a convenient comparison with the work of Daniels et al.,[6] we choose the older definition of the plateau modulus as $G_0^N = 4\rho RT/5M_e$, which can lead to some strange prefactors later!

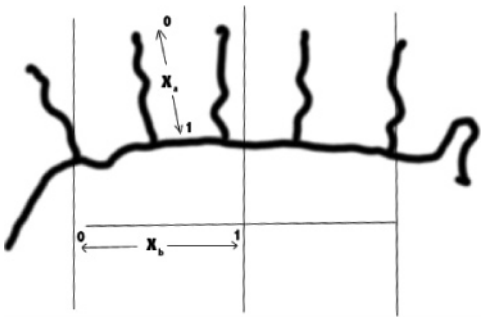

Figure 1. Schematic of an extended simple comb molecule ($q = 5$), with the dimensionless curvilinear coordinates x_a and x_b.

Arm Relaxation. All comb relaxation processes can be derived from the dynamic dilution model.[5,6,11] The relaxation time scales of the arms is given by eq 3, which is derived by allowing the early Rouse-like relaxation modes of the chain, τ_{ae}, to cross over to the slower "activated" relaxation of the star arms, τ_{al}.

$$\tau_a(x_a) = \frac{\tau_{ae}(x_a)e^{U_a(x_a)}}{1+\tau_{ae}(x_a)e^{U_a(x_a)}/\tau_{al}(x_a)} \qquad (3)$$

The early relaxation time is given by the equation[5]

$$\tau_{ae}(x_a) = \frac{225\pi^3}{256} s_a^4 x_a^4 \tau_e \qquad (4)$$

Here τ_e is the Rouse relaxation time of a chain of one entanglement length ($M = M_e$), which depends on the particular polymer chemistry. The activated relaxation time uses the late time formula for star polymers from the Milner and McLeish theory, modified for the presence of both arm and backbone material, similar to theories for H-polymers[5,11]

$$\tau_{al}(x_a) = \frac{\tau_e s_a^{3/2}\left(\frac{2\pi^5}{15}\right)^{1/2} e^{U_a(x_a)}}{x_a(1-\phi_a x_a)^{\alpha}} \quad (5)$$

See appendix A for a discussion of the first passage time calculation used to derive eq 5. The effective potential energy felt by the chain as it retracts into the tube, U_a, is[11]

$$U_a(x_a) = \frac{15 s_a(1-(1-\phi_a x_a)^{\alpha+1}(1+(1+\alpha)\phi_a x_a))}{4(1+\alpha)(2+\alpha)\phi_a^{\,2}} \quad (6)$$

Backbone Relaxation. Once the arm retraction time at the branch point $\tau_a(1)$ is known, the relaxation time along the comb backbone can be calculated. For contour length fluctuations, the backbone behaves as a star arm modified with additional friction due to the arms at every branch point. The calculation again utilizes a function that crosses over from an early relaxation time, $\tau_{be}(x_b)$, to a late one, $\tau_{bl}(x_b)$. The terminal relaxation time is the reptation time of the backbone itself, diffusing inside the dilated backbone tube. Segments are relaxed by whichever disentanglement process is faster, contour length fluctuation (CLF) or reptation. Thus, when the reptation time is calculated to be less than the relaxation time by fluctuation for any segment, then its relaxation is assigned to the reptation time. This is the terminal relaxation time.

The only additional molecular physics not known a priori, but necessary to any dynamics involving diffusion of branch points, is the fraction of a (dilated) tube diameter by which a branch hops when its arm undergoes a complete retraction. We denote this fraction by $1/p$, leading to an expression for the branch point diffusion constant $D_e = a_e p^2/2\tau_a(1)$, where $a_e = a\phi_b^{\alpha/2}$ is the diameter of the dilated tube at the time scale of full arm retraction. Here, as elsewhere,[6] we take $p = 1/\sqrt{12}$, although recently a fuller treatment of the relaxation of branched polymer melts indicates that p^2 could be as low as 1/40.[30]

The derivation proceeds by calculating the diffusion of branch points in a similar way to beads in the Rouse model.[1,6] The form of the early-time relaxation of backbone segments differs depending on whether it is dominated by the diffusion of just one branch point or several. The first case applies to H-polymers, pom-poms, and lightly branched combs and the second to highly branched combs. For a comb to be classed as heavily branched,[6] it must have more than one branch point in the part of the backbone relaxed by fluctuation, i.e., $q > (2M_b/M_e^*)^{1/2}$, where the renormalized entanglement molecular weight which includes relaxed comb backbone is $M_e^* = M_e(\phi_b(1-x_c))^{-\alpha}$. In either case, the backbone relaxation time as a function of distance from the first branch to the center of the molecule from CLF takes the crossover form

$$\tau_b(x_b) = \frac{\tau_{be}(x_b)e^{U_b(x_b)}}{1+\tau_{be}(x_b)e^{U_b(x_b)}/\tau_{b1}(x_b)} \quad (7)$$

The curvilinear diffusion constant of the branch point in the case of a pom-pom[11] is $D_{b,eff} = p^2a^2/(2(f-1)\tau_a(1))$. Here, f is the functionality or the number of free arms at one branch point and a is the dilated tube diameter. Early stress relaxation occurs by free diffusion of the branch point with relaxation time[11] $\tau_{be}(x_b) = x_b^2 L_{b,eff}^2/8D_{b,eff}$. Substitution gives the early time relaxation of pom-poms as

$$\tau_{be}(x_b) = \frac{25}{64p^2} f s_b^{\,2} x_b^{\,2} \tau_a(1)\phi_b^{\,2\alpha} \quad (8)$$

For the case of lightly branched combs the friction is concentrated at the first branch points at either end of the chain because of the two dangling arms. So effectively the early time eq 8 for an H-polymer is valid with $f = 2$. The early relaxation times of the light combs are the same as the H-polymer and are proportional to x^2; this is due to the friction being concentrated at the outermost branch points.

For highly branched combs we calculate the early diffusion of branch points in a similar way to beads in the Rouse model.[1,6] We treat the branch points as beads and renormalizing the Kuhn length (see Appendix B). The early time CLF is dominated by highly coupled backbone frictional blob dynamics arising from more than one branch point. This is better approximated by

$$\tau_{be}(x_b) = \frac{375\pi}{8192p^2} q s_b^{\,3} x_b^{\,4} \tau_a(1)\phi_b^{\,3\alpha} \quad (9)$$

The late relaxation time for CLF differs from Daniels et al.[6] and is corrected to give

$$\tau_{bl}(x_b) = \frac{25 s_b^{\,2}\phi_b^{\,2\alpha} q\tau_a(1)e^{U_b}\sqrt{\frac{2\pi}{U_b''(x_b=0)}}}{8U_b'(x_b)p^2} \quad (10)$$

The need for this correction arises from an incorrect factor of 2 in ref 6. The correct first passage time calculation is given in Appendix A. The effective potential felt by the backbone for retraction is[6]

$$U_b(x_b) = \frac{15 s_b\phi_b^{\,\alpha}(1-(1-x_b)^{\alpha+1}(1+(1+\alpha)x_b))}{8(1+\alpha)(2+\alpha)} \quad (11)$$

Note the prefactor is smaller by a factor of 2 compared to the prefactor in eq 6, since in this expression the backbone is treated as a two-armed star of length $s_b/2$.

The backbone fluctuation time increases rapidly with distance from the chain end, and once this time exceeds the reptation time, then reptation becomes the preferred relaxation method. The backbone reptation time in *both* the cases of lightly and highly branched combs is

$$\tau_{rep} = \frac{25(1-x_c)^2 s_b^{\,2}\phi_b^{\,2\alpha}\tau_a(1)q}{8\pi^2 p^2} \quad (12)$$

where x_c is the dimensionless distance into the tube at which reptation becomes faster than fluctuation, calculated self-consistently by solving[12] $\tau_{rep}(x_c) = \tau_b(x_c)$. Equation 12 is derived from the standard expression $\tau_{rep} = L_e^2(1-x_c)^2 s_b/(\pi^2 D_{rep})$, with the reptation diffusion constant found by addition of the drag from each branch point, $D_{rep} = D_e/q$. We use numerical trapezium integration[13] to compute the Fourier transforms in eq 2 (to evaluate $G'(\omega)$ and $G''(\omega)$).[11]

High-Frequency Theory. The chain dynamics within the confines of the tube are governed by Rouse and longitudinal relaxation modes.[23] The contribution to the shear relaxation

modulus is given by a sum of the longitudinal modes and Rouse modes from both the comb arms and the backbone:

$$G_{\mathrm{comb}}(t) = \frac{G_0^N \phi_a}{s_a}\left[G_{\mathrm{Rouse,a}}(t) + \frac{G_{\mathrm{long,a}}(t)}{5}\right] + \frac{G_0^N \phi_b}{s_b}\left[G_{\mathrm{Rouse,b}}(t) + \frac{G_{\mathrm{long,b}}(t)}{5}\right] \quad (13)$$

The imaginary part of the Fourier transform gives the loss modulus and the real part of the Fourier transform gives the storage modulus. For the arms of the comb polymer the contributions to the modulus are

$$G_{\mathrm{long,a}}(t) = \sum_{p=1}^{(5s_a/4)-1} \exp\left(-\frac{p^2 t}{s_a^2 \tau_e}\right) \quad (14)$$

$$G_{\mathrm{Rouse,a}}(t) = \sum_{p=5s_a/4}^{\infty} \exp\left(-\frac{2p^2 t}{s_a^2 \tau_e}\right) \quad (15)$$

The factors of $^5/_4$ in the limits of the summations arise from the Milner−McLeish definition of the number of entanglements (see ref 26 for details). The sub-tube Rouse modes have a relaxation time of half of τ_e. This arises because, for a 3-dimensional chain, the stress is the second moment of the chain tangent correlation function, and this second moment relaxes with half the Rouse relaxation time. For the longitudinal modes, it was as shown in ref 23 that the projection of the chain on to a 1D tube means that there is no factor of $^1/_2$ in the relaxation time. In the case of the backbone the presence of branches suppresses longitudinal Rouse motion for modes that are less than q; therefore, the backbone contributions are

$$G_{\mathrm{long,b}}(t) = \sum_{p=q}^{(5s_b/4)-1} \exp\left(-\frac{p^2 t}{s_b^2 \tau_e}\right) \quad (16)$$

$$G_{\mathrm{Rouse,b}}(t) = \sum_{p=5s_b/4}^{\infty} \exp\left(-\frac{2p^2 t}{s_b^2 \tau_e}\right) \quad (17)$$

Polydispersity Effects. We consider polydispersity in the comb arms in a more thorough way than the simple method suggested in Daniels et al.[6] A method of averaging over many comb structures, in which each comb was treated independently, was used by Kapnistos et al.[22] to deal with polydispersity of arm length, backbone length, and arm number. However, this method does not account for the cooperative effect of chain dilution, which is known to have a significant effect on the relaxation of entangled polymers, particularly for branched architectures. In branched polymers, the relaxation of a particular chain is strongly influenced by the motion of its surrounding chains. A detailed account of moderate polydispersity in arm length was developed by Frischknecht et al.[25] This treatment accounts for interchain cooperative relaxation through the dynamic dilution hypothesis and can be applied to H-polymers and combs. In this approach a single branch point hopping time is found by computing the mean retraction time from a dynamic dilution calculation over the whole arm molecular weight distribution. The resulting hopping time is always longer than the monodisperse case. We note that both of these methods are relatively simple analytical modifications to an essentially monodisperse theory. In contrast, Park et al.[28] and Shanbhag and Larson[29] have recently examined polydispersity in branched polymers using hierarchical calculations and slip-link simulations. They demonstrate that a single very mobile branch point can dominate the relaxation of an H-polymer backbone, and so in this case polydispersity tends to decrease the terminal time. However, this result would appear to be particular to the H-polymer architecture. For highly branched combs, the influence of very mobile branch points will be diminished since, if a branch point is pinned between slower branch points in a backbone, it must still wait for the slow branch points around it to relax. In this instance the preaveraged approach to polydispersity of Frischknecht et al.[25] combined with our new approach to the end branch points in combs (see Appendix C) would seem to be applicable and computationally cheaper. Many of these points hinge critically on the debate over the physics of branch point motion and on how well the melt polydispersities are known. These issues indicate the need for further theoretical insight into branch point motion, combined with well-chosen experiments to distinguish between different approaches.

Table 2. Polybutadiene Comb Polymer Structural Parameters

comb	q	M_a (kg mol^{-1})	ϵ_a	M_b (kg mol^{-1})	G_0 (MPa)	M_e (g mol^{-1})	τ_e (s) at 27.5 °C
PBC 5	8	11.9	1.04	63.9	1.6	1800	2.2×10^{-7}
PBC 6	9	28.8	1.03	60.5	1.6	1800	2.2×10^{-7}
PBC 7	8.4	22.7	1.07	61.4	1.6	1800	2.2×10^{-7}
PBC 9	8	20.1	1.01	81.8	1.8	1800	2.2×10^{-7}
PBC 10	7	14.9	1.05	53.8	1.6	1800	2.2×10^{-7}
PBC 11	8.2	22.7	1.05	62.7	1.8	1800	2.2×10^{-7}

We used the Frischknecht et al. correction to arm polydispersity for a melt of arms in an immobile volume fraction from the comb backbones. This approach identifies two rheological effects of polydispersity: (1) an increase to the mean longest relaxation time of the arms at the branch point $\tau_a(1)$ and (2) a correction to the arm contribution to the relaxation modulus $G(t)$, a more subtle change making the features in the rheology less sharp. The increase to the mean longest relaxation time of the arms at the branch point is given by[25]

$$\langle \tau_a \rangle = \tau_{a0} \exp[\nu^2 \phi_b^2 s_a^2 \epsilon_a/2] \quad (18)$$

The correction to the relaxation modulus of the arms itself is

$$\frac{\mathrm{d}G(t)}{G_N^0(1+\alpha)} = \int_0^\infty \mathrm{d}y \, \frac{\phi_a}{\sqrt{y s_a}}\left[\phi_a\left(1 - \sqrt{\frac{y}{s_a}}\right)\theta(y - s_a) + \phi_b\right]^\alpha \left[\frac{1}{2} - \frac{1}{2}\,\mathrm{erf}\left(\frac{y - s_a}{\sqrt{2}\Delta}\right) - \theta(y - s_a)\right] \mathrm{e}^{-t/\tau(y)} \quad (19)$$

where $y = s_a x_a^2$ and $\Delta = \sqrt{\epsilon s_a}$. $\theta(y - s_a)$ is a step function. The relaxation time in terms of the new variable y is

$$\ln \tau(y) = \nu \phi_a\left(y - \frac{2y^{3/2}}{3 s_a^{1/2}}\right) + \nu \phi_b y \quad (20)$$

IV. Results and Discussion

Now we compare our predictions to linear oscillatory shear measurements on a range of different comb architectures. Our calculations include, in each case, corrections due to polydispersity and the end branch point motion (see Appendix C). The oscillatory shear response was calculated to evaluate the storage and loss modulus, $G'(\omega)$ and $G''(\omega)$. For details of the synthesis of the combs refer to ref 4 and for the experimental rheology to ref 6. We used the following parameters: $M_e = 1800$ g mol^{-1}, $G_0 = 1.6$ MPa, and $\tau_e = 2.2 \times 10^{-7}$ s at a temperature of 27.5 °C. We used the dilution exponent $\alpha = {}^4/_3$. For the materials

PBC 9 and PBC11, it was necessary to increase the plateau modulus; however, this variation is within commonly occurring experimental error in absolute values of moduli. We were able to describe the majority of the combs using the structural parameters derived from the analysis of the chemistry of the materials in ref 6. One exception was that we had to increase the arm polydispersity in comb 10 to 1.05 (from 1.01). Using corrections to the original comb model, we have been able to successfully describe the rheology of the polybutadiene combs using the original chemistry values of the structure. We were also able to capture quantitatively the effects of polydispersity in a way consistent with tube theory. Figure 2g shows a comparison of $G''(\omega)$ for the most polydisperse comb studied, PBC7. The most accurate description of the experimental data is with the cooperative treatment of polydispersity. We compare this to the cases with no polydispersity and to the result by averaging over many chains.[7] Clearly the effect of taking the average of many chains does not accurately describe the rheology of the material. We note here that alternative approaches to polydispersity using either hierarchical relaxation models[28,30] or slip-link simulations[29] have produced successful predictions for polydisperse branched systems.

We now use the model to make predictions of linear comb rheology for a wider class of materials than are currently available synthetically. For all calculations that follow we assume perfectly monodisperse molecular structure and an equal separation between branch points, and we ignore the end branch point correction in Appendix C. We calculate the rheology of a material similar to polyethylene by using the following parameter values: $\tau_e = 1.562 \times 10^{-8}$ s, $M_e = 1250$ g mol^{-1}, and $T = 170$ °C.

In the following discussion, we keep one of the following parameters constant while varying the other two: arm length, backbone length, and number of arms. In this case the backbone length is measured form the first branch point to the last branch point (ω). As $G''(\omega)$ shows more of the structural features than $G'(\omega)$, we shall only consider this in the following discussion.

We can see in Figure 3 that increasing the length of the arms gives the comb loss modulus a very large shoulder feature to the data as in the case of star-shaped polymers. The prominence of the backbone reptation "hump" decreases in size due to the action of dilution of the backbone volume fraction by the presence of increased arm material. The terminal relaxation time is very strongly controlled by the longest relaxation time of the arms.

The variation of backbone length while keeping the arm length and arm number constant also extends relaxation features to lower frequency, although not as dramatically as does arm length. As backbone length was increased, we found that the reptation "hump" becomes more prominent in size as the backbone volume fraction dominates.

As the number of arms increases relative to the other parameters, the backbone relaxation features are smoothed out due to a decrease in backbone volume fraction. In fact, with combs that are very highly branched, the reptation "hump" can almost disappear entirely. This is interesting in understanding the shape of the loss modulus of highly branched LPDE that does not display any humps whatsoever, suggesting that multiply branched, short arms act to dilute the rest of the molecule(s), in a similar, but more radical, way than combs. From the above analysis, we can conclude that the lengths of the arms are the most sensitive controlling feature of the shear rheology. This is because the relaxation time at the branch point has an exponential dependence on the length of the arms but also due to the range of intermediate relaxation times controlled by this dependence. The longest arm relaxation time also sets the relaxation time of the backbone. The number of branches and the backbone dynamics are more important in extensional flow because they act to serve as friction points that enhance the stretch of backbone sections as in the pom-pom model[15−17] that leads to extensive strain hardening behavior in extensional flow; this is, however, beyond the scope of this paper.

Calculation of Zero-Shear Viscosity vs Molecular Weight. From the calculation of $G''(\omega)$ we can calculate the zero-shear viscosity by taking the limit of zero strain rate.[1]

$$\eta_0 = \lim_{\omega \to 0} \frac{G''(\omega)}{\omega} \tag{21}$$

For the purposes of this calculation, we used a limiting value of the frequency: 10^{-8} s^{-1}. The zero-shear viscosities of polyethylene linear star and comb polymers were calculated for several molecular weights.

Figure 6 shows the zero-shear viscosity calculated for polyethylene combs vs molecular weight. Parameters values used were for polyethylene, $\tau_e = 9.5 \times 10^{-9}$ s and $M_e = 1150$ g mol^{-1}, which were calculated for polyethylene at 190 °C. The value of τ_e was calculated using equations derived from Rouse theory,[14] and the value of M_e was chosen to give agreement with the linear power law and the corrected Milner−McLeish model for linear polymers.[12,24] The zero-shear viscosity points were calculated using a loop over arm lengths, s_a, backbone lengths, s_b, and the number of branches in the comb, q. Calculations were performed over the following ranges: $2 < s_a < 10$, $6 < s_b < 100$, $6 < q < s_b$. q was chosen to be no more than s_b to ensure there is at least one entanglement between branch points. The results were calculated for polyethylene at 190 °C in order to compare the result to the power law for linear polyethylenes,[18] plotted as a line in Figure 6 which has the equation

$$\eta_0 = 5.8 \times 10^{-14} M_W^{3.41} \tag{22}$$

We calculated the zero-shear viscosities of a notional 3-armed star polymer of length up to 40 entanglements for comparison to the comb data. Note that stars with more arms than three act to shift this curve to the right due to increasing molecular weight. To check that the parameter values of τ_e and G_0 used in the above calculations were correct, we compared the results with the Milner−McLeish model for linear polymers,[12] and a good agreement was found with eq 22.

The result of Figure 6 is significant in that, experimentally, metallocene-catalyzed polyethylenes are shown to deviate from the power law line dramatically in the same way that the model combs do. The most comprehensive results for this are to be seen in the thesis of Gabriel and subsequent papers.[19,20] In the literature, this has been described as the material possessing "starlike" branching, but it can also be obtained by comb configurations. We can obtain more insight into the effect of molecular structure on the zero-shear viscosity by decomposing Figure 6 into domains with specific values of the parameters s_a, s_b, and q.

From the set of zero-shear viscosities calculated for all the comb structures in the ranges $2 < s_a < 10$, $6 < s_b < 100$, and $6 < q < s_b$, we plot only constant values of one of the variables to gain insight into the dependence of the zero-shear viscosity with comb structure. Figure 7a shows zero-shear viscosities vs molecular weight for which q is constant with values 10, 50, and 100 arms. We can clearly see that the effect of adding more

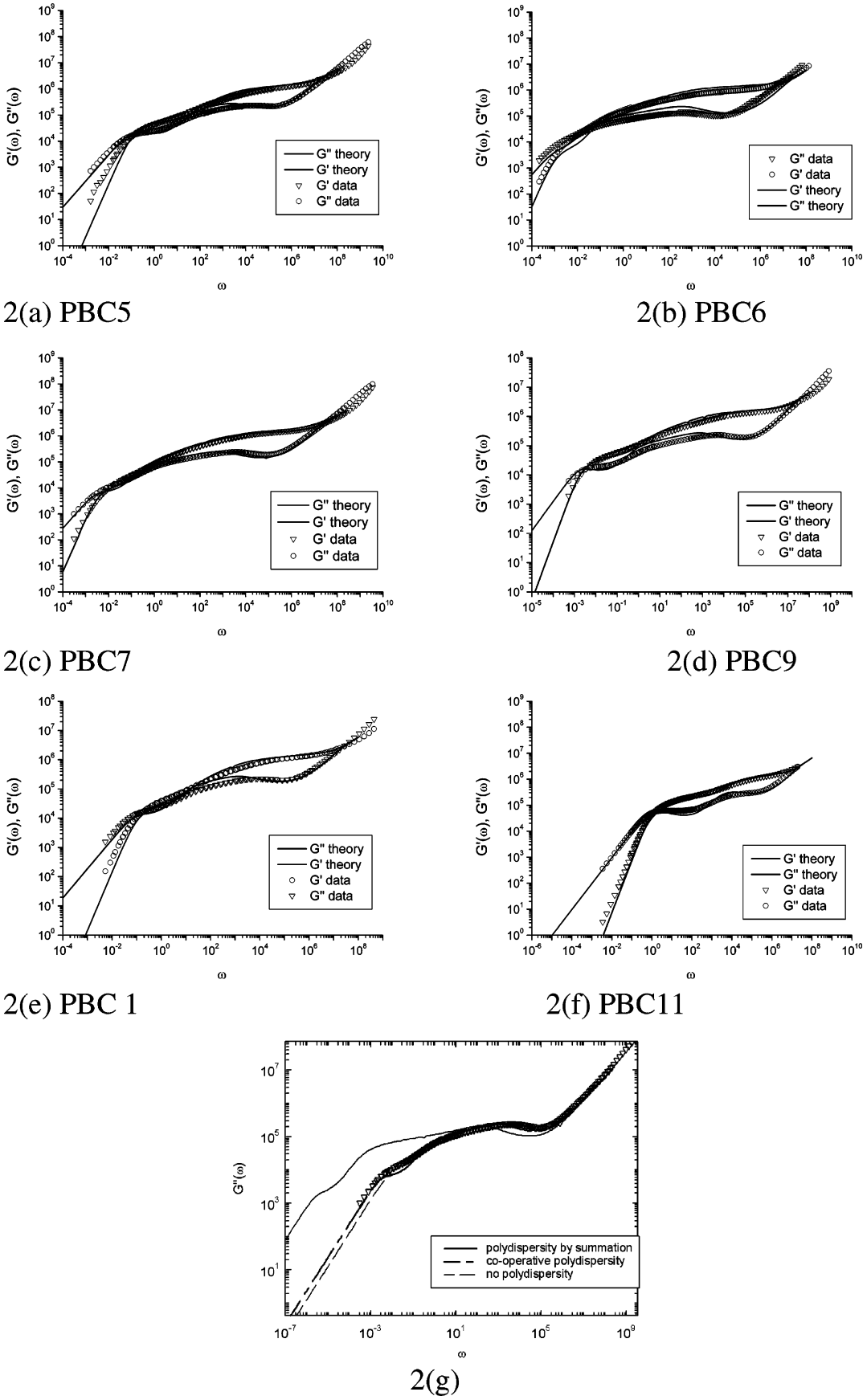

Figure 2. Storage and dissipation moduli of polybutadiene combs for the theory (lines) with experimental data (circles and triangles). Comb structural parameters are the chemistry values[6] of the comb structure with little adjustment at $T = 27.5$ °C. Materials are (a) PBC5, (b) PBC6, (c) PBC7, (d) PBC9, (e) PBC10, and (f) PBC 11. (g) shows a comparison of $G''(\omega)$ for the most polydisperse comb, PBC7, for the successful fitting of the data with the cooperative treatment of polydispersity (dark dash) compared to the cases with no polydispersity (light dash) and to the result of averaging over many chains (solid line).

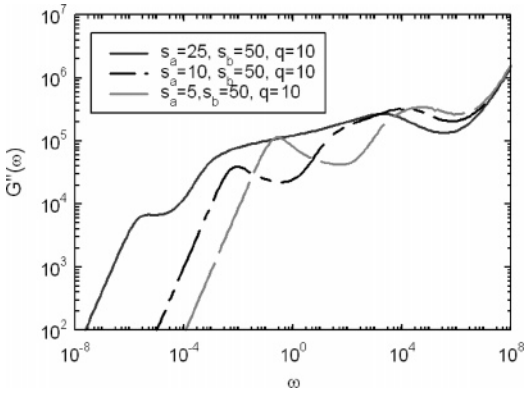

Figure 3. Loss modulus calculated for monodisperse comb polyethylenes with varying arm length in numbers of entanglements and 10 arms.

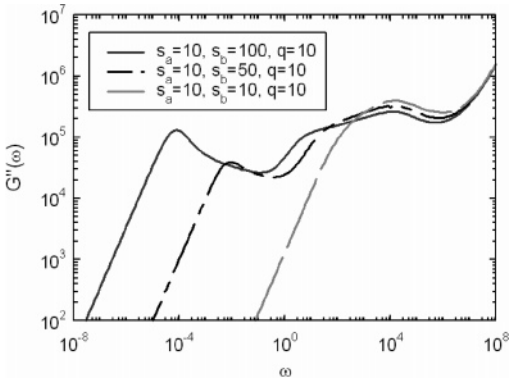

Figure 4. Loss modulus calculated for monodisperse comb polyethylenes with varying backbone length.

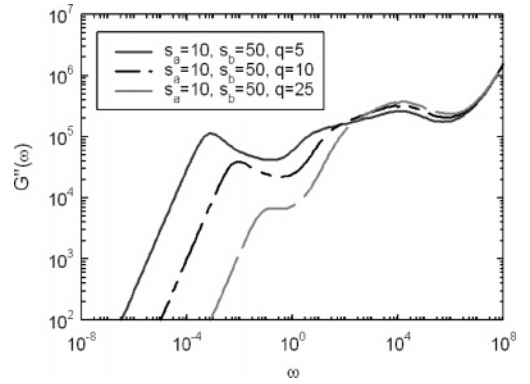

Figure 5. Loss modulus calculated for monodisperse comb polyethylenes with varying arm number.

arms to comb polymers increases the molecular weight and acts to reduce the zero-shear viscosity in a dilution effect. Figure 7b shows zero-shear viscosities vs molecular weight with constant values of arm length of 2, 6, and 10 entanglement segments, as the backbone length and number of arms are varied. In the case of the shortest arms where $s_a = 2$ entanglement segments, the data lie in a domain both above and below the power law line for linear polymers. As the arm length is increased, this domain shifts along the molecular weight axis but also the spread in the range of zero-shear viscosity increases (in height). The data lies on either side of the linear power law line. Figure 7c shows zero-shear viscosities vs molecular weight data with constant $s_b = 10$, 20, 50, and 100 entanglements. It is apparent that the backbone length has a similar effect to the arm length. As the backbone length is increased, the domain of the data shifts along the molecular weight axis, and again the

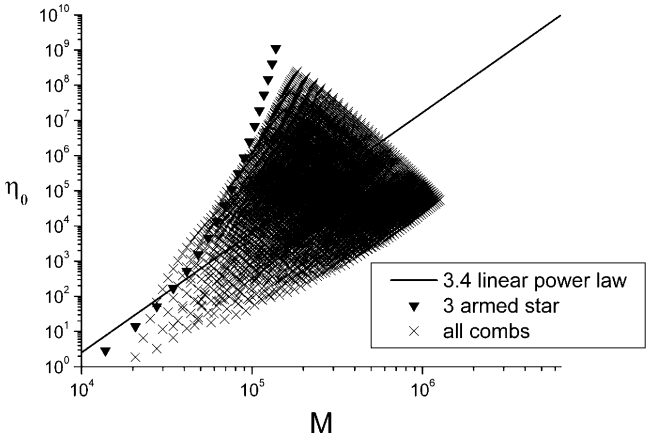

Figure 6. Predicted zero-shear viscosity vs molecular weight of polyethylene combs (crosses) with varying arm, backbone length, and arm number compared to the power law relation for linear HDPE. Triangular points are 3-armed stars.

spread in the range of zero-shear viscosity increases (in height). However, we must note that the effect of the arm molecular weight is stronger that the backbone length because of the relative values of the number of entanglement segments (lengths). From the above analysis of our data, it seems that the arm length and the backbone length can vary substantially the position of the zero-shear viscosity for a given molecular weight. This is because the one of the parameters is being varied while the other is held constant. By further analyzing the individual data points, we found that the highest zero-shear viscosities are obtained with combs that have long arms *and* long backbones and with few arms. We find that the combs with short backbones and short arms with many arms lie under the 3.4 index power law line obeyed by linear polymers. Increasing the arm length and the backbone length lifts the zero-shear viscosity upward away from the power law line and to the right along the molecular weight axis. The number of arms shifts the molecular weight in a translation to the right along the M axis and reduces the zero-shear viscosity, as many arms act to enhance dynamic dilution (through ϕ_a). It is interesting that many of the points lie below the linear 3.4 power law line of linear polymers, although it should be bourn in mind that the choice of M_e affects the vertical shift in the model. Interestingly commercial, highly branched materials such as LDPE can have zero-shear viscosities above the power law line but more often are to be found well below it.[19,20] This makes sense if the idea that many short arms having a diluting effect on the zero-shear viscosity is correct. We also note that work by Auhl et al.[27] demonstrates a reduction in zero-shear viscosity by the effect of increasing arm number by the irradiation of polypropylene.

From the decomposition of all the calculated data, we can summarize: The length of both comb and star polymer arms dictates the height above the linear power law of the zero-shear viscosity with an exponential dependence and is therefore the key variable for control of zero-shear viscosity. The length of the backbone also contributes to a horizontal and vertical shift of the zero-shear viscosity as it increases but has a weaker dependence than the arm length. The number of arms dominates a horizontal shift and a vertical reduction in the zero-shear viscosity in molecular weight.

On analysis of the data we found that the combs that lie on the same curve as the 3-armed star are the combs with the longest arms *and* longest backbones with the fewest number of arms ($q = 6$). Interestingly, the lengths of the arms of the combs,

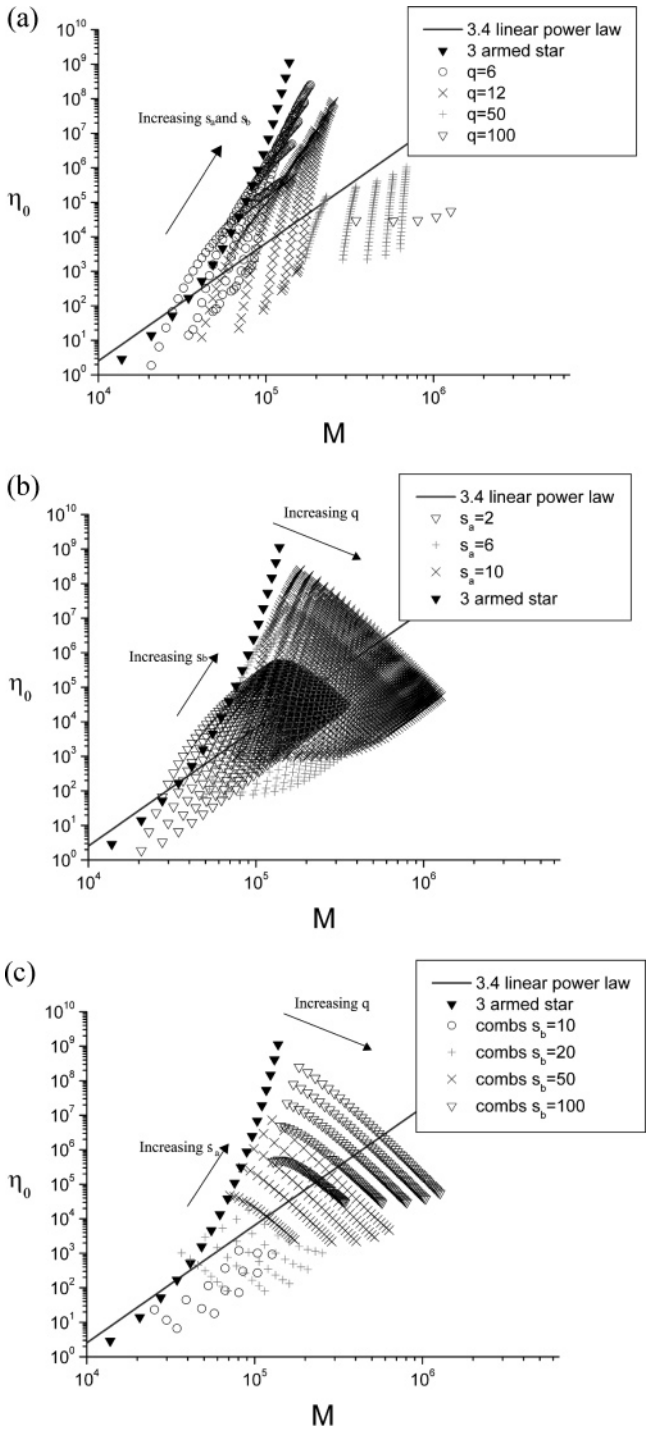

Figure 7. (a) Variation of η_0 with molecular weight for constant q = 10, 50, and 100, while s_a and s_b are varied. (b) Variation of η_0 with molecular weight for constant s_a = 2, 6, and 10 entanglement segments, while s_b and q are varied. (c) Variation of η_0 with molecular weight for constant s_b = 10, 20, 50, and 100 entanglement segments, while s_a and q were varied.

which lie on this star curve, are less than the stars because the long backbones enhance the zero-shear viscosity. We can formulate the question: Given a specific zero-shear viscosity for a multiply branched metallocene-catalyzed material, is it possible to determine the molecular structure from this map of comb structures? Unfortunately, not, as even in this family of monodisperse architectures, many different structures can give equivalent zero-shear viscosities. It is clear by the density of points (of all the combs) that several structural topologies share the same value of the zero-shear viscosity. However, if the specific length of arms is known, which it can be, in the case of polymacromers, then it could enable a determination of structure.

We also repeated this calculation of zero-shear viscosity with pom-poms instead of combs. We found that the pom-poms lie in an identical area to the comb polymers. This knowledge outlined above means that polymer structure design could result in desired material properties, as the zero-shear viscosity of materials is an important attribute in material processing and solid-state mechanics.

Analytical Relation of the Zero-Shear Viscosity and Structural Parameters. The zero-shear viscosity of a polymer melt is approximately calculated from the product of the plateau modulus and the terminal relaxation time. For a comb, this is the backbone reptation time.

$$\eta_0 = G_0\tau_{\text{rept}} \tag{23}$$

Substituting the comb reptation time from eq 12 gives

$$\eta_0 \propto G_0(1 - x_c)^2 s_b^{\,2}\phi_b^{\,2\alpha}\tau_a(1)q \tag{24}$$

Using our melt expressions for $\tau_a(1)$, we found that the approximate form of (23) could be made quantitative in comparison to the full integral over $G(t)$ by the introduction of a numerical prefactor. The resulting approximate analytical expression for the viscosity for polyethylene combs (190 °C) is

$$\eta_0 \approx \frac{1.60G_0 s_b^{\,2}\phi_b^{\,8/3} q\tau_e s_a^{\,3/2} e^{[27s_a(1-(1-\phi_a)^{7/3}(1+7\phi_a/3))]/112\phi^2_a}}{(1-\phi_a)^{4/3}} \tag{25}$$

V. Conclusions

Using corrections to the original comb model, we have been able to successfully describe the rheology of the monodisperse polybutadiene combs using the original chemistry values of the structure alone. Our choice of α was $^4/_3$, whereas other comb models use α as being equal to unity. At this level of detail, the choice of $\alpha = 1$ does not agree as well with the experimental data when chemistry-derived parameter values are used. We were able to qualitatively capture the effects of polydispersity in a way consistent with tube theory, where the cooperative effect of chain dilution from arms of variable lengths in a network of slower entangled material must be taken into account. The influence the backbone extremities giving rise to two effective arms of different lengths at the end branch point was also accounted for quantitatively within the dynamic dilution framework.

From the comb theory we derived a simple analytical equation to evaluate the zero-shear viscosity of monodisperse comb polymers, in terms of structural variables of arm length, backbone length, and the number of branches. We demonstrated that the zero-shear viscosity is exponential in arm length and arm volume fraction. The zero-shear viscosity varies with the square of the backbone length and linearly with the number of branches, although there is also a q dependence in the volume fractions. The length of comb polymer arms is therefore the key variable for control of zero-shear viscosity. The length of the backbone also contributes to a horizontal and vertical shift of the zero-shear viscosity as it increases but has a weaker dependence than the arm length. Increasing the number of arms will increase the molecular weight but reduce the zero-shear viscosity. This model relates branched polymer molecular structure to a rheological variable that can be measured by

simple rheology. It is hoped that this work will enable design of materials through controlled chemistry and catalysis in the future.

Acknowledgment. We thank the microscale polymer processing consortium (μPP1(GR/M597474/01) and μPP2(GR/T11807/01)), the EPSRC, and the Dutch Polymer Institute for financial support. We thank Dr. Alexei Likhtman for useful discussions; we are very grateful to S. M. Park and Prof. Ron Larson for drawing attention to errors in the prefactors of previously published backbone relaxation time equations.

Appendix A. First Passage Time Calculation

In this appendix, we discuss an analytic approximation, introduced by Milner and McLeish,[5] that is frequently used to describe the arm relaxation time in branched polymer melts. The arm relaxation time is the first passage time of a particle diffusing in an effective potential, $U(x)$. This problem reduces to evaluation of a double integral

$$I(x) = \int_0^x dy \exp[U(y)] \int_{-\infty}^{y} dz \exp[-U(z)] \qquad \text{(A1)}$$

Frischknecht et al.[25] suggest the following approximation

$$I(x) \approx \frac{\exp[U(x)]}{U'(x)} \sqrt{\frac{2\pi}{U''(x=0)}} \qquad \text{(A2)}$$

which is valid when $\exp[U(x)] \gg 1$, i.e., deep retractions, and when $U'(x)$ is sufficiently larger than zero. In these limits the integral over z is dominated by the region close to zero so $U(z) \approx U''(0)z^2/2$, and the range of integration can be taken to be $-\infty$ to ∞. The integral over y is dominated by the potential close to the upper limit, x, so $U(y) \approx U(x) + (y - x)U'(x)$. These approximations allow the integration to be performed analytically, leading to eq A2. Several publications erroneously have the factor of 2 in the denominator inside the square root rather than in the numerator as above.[5,6]

Appendix B. Derivation of Early Fluctuation Time for Highly Branched Backbone

Here we derive the early fluctuation time of a highly branched comb backbone. The calculation proceeds by analogy with the sub-Fickian diffusion of a one-dimensional Rouse chain. For comb backbones, the expressions for both the frictional drag and the tube diameter are changed, but the underlying physics is the same. The friction of the backbones is renormalized since the drag is dominated by the friction at the branch points, of which there are q along the whole chain. The entanglement network is also renormalized since all arm segments act as solvent at these time scales meaning that entanglements can only be formed with other backbones. Equation 6.107 from Doi−Edwards,[1] which describes the sub-Fickian diffusion of an entangled Rouse chain, can be written as

$$\langle \Delta R^2 \rangle = \frac{4}{3}\left(\frac{3}{\pi}\left(\frac{Nb^2}{\zeta N}\right) k_B T t\right)^{1/2} \qquad \text{(A3)}$$

We identify ζN as the total drag of the chain, which for our renormalized chain is $\zeta_{bp} q$, where ζ_{bp} is the drag of a single branch point. We also substitute in $Nb^2 = L_e a_e$, where L_e and a_e are respectively the renormalized backbone primitive path length and tube diameter in the entanglement network formed by backbones ($a_e = a\phi_b^{\alpha}/2$). Thus

$$\langle \Delta R^2 \rangle = \frac{4}{3}\left(\frac{3}{\pi}\left(\frac{L_e}{\zeta_{bp} q}\right) a_e k_B T t\right)^{1/2} \qquad \text{(A4)}$$

We note here that the end displacement depends only on the friction per unit length of primitive path and not the chain length, as we expect for early time fluctuations. The friction of a branch point can be obtained from an Einstein relation, $\zeta_b = k_B T/D_e$, where D_e is the effective diffusion constant of the renormalized backbone ($D_e = a_e p^2/2\tau_a(1)$). Inserting these expressions, using $\langle \Delta R^2 \rangle \approx (x_b L/2)^2$ and the approximation that eq A4 can be inverted to give a time scale, leads to the final expression

$$\tau_{be}(x_b) = \frac{375\pi}{8192 p^2} q s_b^{\,3} \phi^{3\alpha} x_b^{\,4} \tau_a(1) \qquad \text{(A5)}$$

where we also used $a^2 = {}^4/_5 N_e b^2$.

Appendix C. End Branch Point Calculation

In this appendix we derive a correction to the theory outlined in the main paper to account for the situation illustrated in Figure 8. The section of backbone between the free end and the first

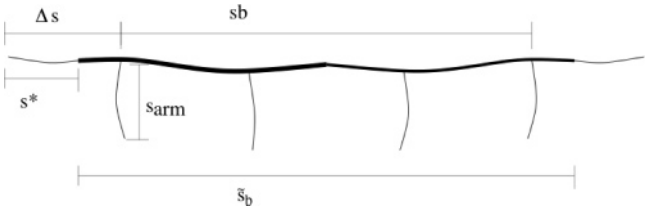

Figure 8. A comb polymer with two different arms lengths at the end branch point. In this case $\Delta s > s_{arm}$ and part of the longer arm is incorporated a renormalized backbone.

branch point, Δs, is able to act as arm material since it has a free end. In general, this end arm will be a different length to the grafted arms. Furthermore, if we assume that the branches are evenly spaced, Δs may be longer or shorter than s_{arm}, depending on the comb's structural parameters. We contrast this calculation with the derivation in the main paper, in which we assumed that all arms are the same length. Our results demonstrate that, for the materials considered in this study, the correction is noticeable but small.

We begin by calculating the star arm retraction for a blend of two different arm lengths and a fraction of fixed backbone material. This is a slightly more general case of a similar calculation for asymmetric stars made by Frischknecht et al.,[25] and their approach can be adapted to model an asymmetric comb end. We denote the arm length as s_s and s_l for the short and long arms and the volume fractions are Φ_s, Φ_l, and Φ_B for the short arms, long arms, and backbones, respectively. We compute the effective potential for each arm using the Ball−McLeish equation. By changing variables to $y = x_i^2 s_i$, for each arm species i, the dependence on arm lengths can be removed to give

$$\frac{d(\ln \tau)}{dy} = \nu \Phi^{\alpha} = \frac{dU_{eff}(y)}{dy} \qquad \text{(A6)}$$

Thus, at the level of the Ball−McLeish equation, it takes the same time for either a long or short arm to retract to a given value of y. We consider two cases separately: before the short arms have retracted ($y < s_s$) and after all short arms have relaxed

($y > s_s$). In each case the unrelaxed volume fraction, Φ, can be written as a function a single variable y. For $y < s_s$

$$\frac{dU_{eff}(y)}{dy} = \nu\left[\Phi_B + \Phi_s\left(1 - \sqrt{\frac{y}{s_s}}\right) + \Phi_l\left(1 - \sqrt{\frac{y}{s_l}}\right)\right]^\alpha$$
$$= \nu\left[1 - \left(\sqrt{\frac{1}{s_s}}\Phi_s + \Phi_l\sqrt{\frac{1}{s_l}}\right)\sqrt{y}\right]^\alpha \quad (A7)$$

with the second line following because $\Phi_B + \Phi_s + \Phi_l = 1$. This is of the same form as eq A2 from Frischknecht et al. so we can use their expressions for the effective potentials (eqs A5 and A6 from Frischknecht et al.). When $y > s_s$, the Ball−McLeish equation becomes

$$\frac{dU_{eff}(y)}{dy} = \nu\left[\Phi_B + \Phi_l\left(1 - \sqrt{\frac{y}{s_l}}\right)\right]^\alpha \quad (A8)$$

which, after integrating and changing variable back to x_l, leads to

$$U_{eff}(x_l) = \frac{2\nu\Phi_l{}^\alpha s_l(1+A)^{\alpha+2}}{(\alpha+1)(\alpha+2)}\left[1 - \left(1 - \frac{x_l}{(A+1)}\right)^{\alpha+1}\left(1 + (\alpha+1)\frac{x_l}{(A+1)}\right)\right] + C \quad (A9)$$

where $A = \Phi_B/\Phi_l$ and the constant of integration, C, is chosen to match the two expressions for the long arm potential at $x_l = \sqrt{s_s/s_l}$. Thus, the relaxation times for both the short and long arms can be computed from their respective potentials, as before, via

$$\tau_i(x_i) = \frac{\exp(U_i(x)}{U_i'(x)}\left(\frac{2\pi}{U_i'(x_i{=}0)}\right)^{1/2} \quad (A10)$$

As before, the crossover equation (4) can be used to include early Rouse fluctuations.

The distance retracted by the long arm in the full retraction time of the short arm is denoted s^* in Figure 8 or x^* for the corresponding fractional distance. By definition, this is given by

$$\tau_l(x_l = x^*) = \tau_s(x_s = 1) \quad (A11)$$

As noted by Frischknecht et al., this crossover does not occur exactly at $x_l = \sqrt{s_s/s_l}$, as suggested by the Ball−McLeish equation, due to the weakly x-dependent prefactor in the expression for τ_i. Therefore, we find x^* by numerical solution of eq A11.

Next we consider the effect of this detailed calculation when $\Delta s > s_{arm}$. Here, the Δs segments are the long arms and the s_a segments become the short arms. The calculation proceeds as above until the long arms have retracted to x^*. At this point it becomes faster for the remaining long arm segments to relax via reptation of the whole backbone. Effectively, these segments have become part of the backbone (see Figure 7). Thus, $\tau_a(1)$, which controls the frictional drag of the branch points, is given by $\tau_s(1)$. With $\tau_a(1)$ determined, we compute the backbone relaxation, counting all long arm material with $x > x^*$ as backbone. Thus, when computing the backbone relaxation, the effective backbone length increases to

$$\tilde{s}_b = s_b + 2(1 - x^*)\Delta s \quad (A12)$$

and the backbone concentration becomes

$$\tilde{\phi}_b = \frac{\tilde{s}_b M_e}{M_w + qM_a} \quad (A13)$$

From this derivation we see a 2-fold effect on the terminal time. $\tau_a(1)$ becomes slightly longer due to the presence of the additional long-lived material in the longer arms which slows the dilution of the entanglement network. Second, the distance the backbone must reptate is increased. Both of these effects tend to enhance the backbone terminal time.

In the opposite case, when $\Delta s < s_{arm}$, we take Δs as the short arm and s_{arm} as the long arm and compute the two arm times, τ_s and τ_l, as above. Once $t > \tau_s$, the two end branch points are able to fluctuate but their range of motion is limited since the other branch points remain pinned. When $t > \tau_l$, the remaining branch points become mobile and full backbone relaxation can proceed. Unlike before, no further renormalization of the backbone length is necessary since all arm material will have relaxed before substantial backbone motion can occur. However, in this case the frictional drag of the two end branch points is reduced since they are connected to a faster relaxing short arm. These branch points have a relaxation time of τ_s, and the remaining $q - 2$ branch points have a relaxation time of τ_l. For deep fluctuations and reptation of this composite backbone, at the level of the Milner−McLeish model,[12] only the total backbone friction is considered, not the arrangement of these frictional points along the backbone. We compute the total backbone friction by summing over all branch points.

$$\zeta_b = \frac{2k_BT}{a_e p^2}(2\tau_s(1) + (q-2)\tau_l(1)) = \frac{2k_BT}{a_e p^2}\tau_l(1)\left(2\frac{\tau_s(1)}{\tau_l(1)} + (q-2)\right) \quad (A14)$$

which is equivalent to renormalizing q

$$\tilde{q} = q - 2\left(1 - \frac{\tau_s(1)}{\tau_l(1)}\right) \quad (A15)$$

This approach is incorrect for the early fluctuations, where the distribution of friction along the backbone does matter. However, these early backbone fluctuations have little effect on the overall relaxation spectrum and even less influence on the terminal time, where the strongest effect of this more detailed calculation is manifested. For $\Delta s < s_{arm}$ the modification tends to reduce the backbone terminal time, as before, through two effects. $\tau_a(1)$ is reduced by the faster dilution of the entanglement network due to the fast relaxing material in the short arms, and the backbone drag is reduced by the renormalization of q.

We now examine the effect of this modification on the terminal behavior of our model predictions for the combs in this study. PBC 11 is the only comb for which $\Delta s > s_{arm}$ and all other combs have $\Delta s < s_{arm}$. To allow the influence of this correction to be seen in isolation, we do not include any polydispersity corrections in these calculations. Figure 9 shows the effect of the modification compared to the assumption that all arm material has length s_{arm} and demonstrates that the change in terminal is relatively small. Similar or smaller shifts occur in all other materials in this study. In Figure 9 the predicted terminal time is a slightly shorter than the experimental value, a gap that is accounted for by the polydispersity correction. All calculations in Figure 2 include the influence of this end correction. The direction and magnitude of these shifts aid the agreement for all of the combs except PBC 5. In this case the predicted terminal time is too low before the correction is

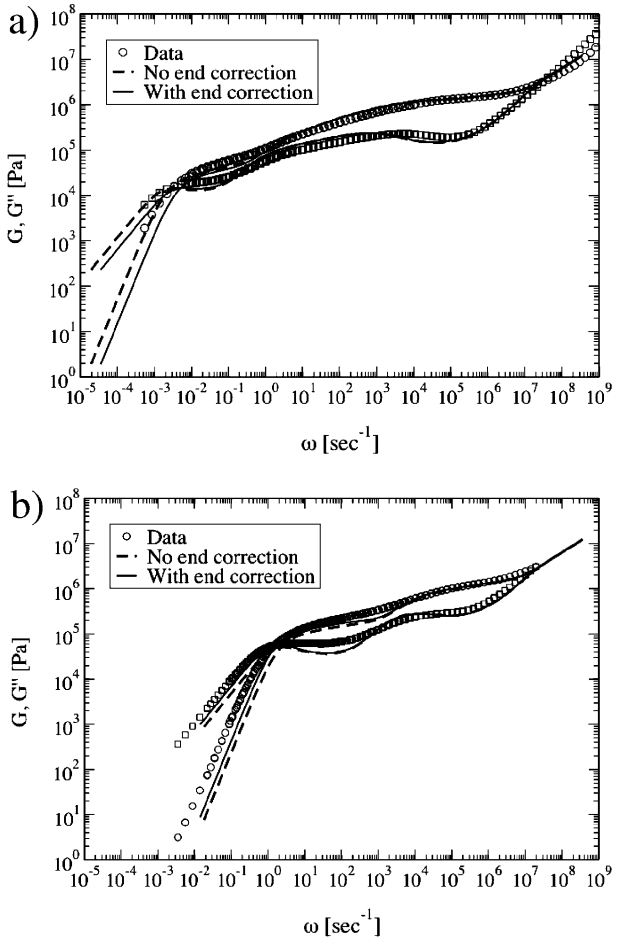

Figure 9. Influence of the end correction on the linear rheology. Dashed lines are for the monodisperse theory outlined in the main part of the article, solid lines show the end correction discussed above, and the shapes are experimental data. (a) shows PBC9 for which $\Delta s < s_{arm}$, and (b) shows PBC11, the only sample for which $\Delta s > s_{arm}$.

applied, and the end branch point correction decreases this further. This may be due to the particularly short arms of this molecule. Overall, the significance of these small shifts should not be overestimated, and our main conclusion is that, for the combs in this study, the influence of the end branch point correction is small.

References and Notes

(1) Doi, M.; Edwards, S. F. *The Theory of Polymer Dynamics;* Oxford Science Publications: New York, 1986.
(2) McLeish, T. C. B. Tube theory of entangled polymer dynamics. *Adv. Phys.* **2002** *51*, 1379−1527.
(3) Roovers, J. E. L.; Bywater, S. *Macromolecules* **1972**, *5*, 384−388.
(4) Fernyhough, C. M.; Young, R. N. The synthesis of and characterization of Polybutadiene and Poly(ethylene-1-butene) Combs. *Macromolecules* **2001**, *34*, 7034−7041.
(5) Milner, S. T.; McLeish, T. C. B. Parameter-Free Theory for Stress Relaxation in Star Polymer Melts. *Macromolecules* **1997**, *30*, 2159−2166.
(6) Daniels, D. R.; McLeish, T. C. B.; Crosby, B. J.; Young, R. N.; Fernyhough, C. M. Molecular Rheology of Comb Polymer Melts. 1. Linear Viscoelastic Response. *Macromolecules* **2001**, *34*, 7025−7033.
(7) Watanabe, H.; Matsumiya, Y.; Osaki, K.; Tube Dilation Process in Star-Branched *cis*-Polyisoprenes. *J. Polym. Sci., Part B* **2000**, *38*, 1024−1036.
(8) Watanabe, H.; Matsumiya, Y.; Inuoue, T. Dielectric and Viscoelastic Relaxation of Highly Entangled Star Polyisoprene: Quantitative Test of Tube Dilation Model. *Macromolecules* **2002**, *35*, 2339−2357.
(9) McLeish, T. C. B. Why, and when, does dynamic tube dilation work for stars?; *J. Rheol.* **2003**, *47*, 177−198.
(10) Ball, R. C.; McLeish, T. C. B. Dynamic Dilution and the Viscosity of Star Polymer Melts. *Macromolecules* **1989**, *22*, 1911−1913.
(11) McLeish, T. C. B.; Allgaier, J.; Bick, D. K.; Bishko, G.; Biswas, P.; Clarke, N.; Groves, D. J.; Hakiki, A.; Heenan, R.; Johnson, J. M.; Kant, R.; Read, D. J.; Young, R. N.; Dynamics of Entangled H−Polymers: Theory, Rheology and Neutron Scattering. *Macromolecules* **1998**, *32*, 6374−6758.
(12) Milner, S. T.; McLeish, T. C. B. Reptation and Contour-Length Fluctuations in Melts of Linear Polymers. *Phys. Rev. Lett.* **1998**, *81*, 725−728.
(13) Press, W. H.; Teukolsky, S. A.; Vettering, W. T.; Flannery, B. P. *Numerical Recipes in C*, 2nd ed.; Cambridge University Press: New York, 1988.
(14) Vega, J. F.; Rastogi, S.; Peters, G. W. M.; Meijer, H. E. H. *J. Rheol.* **2004**, *48*, 663−678.
(15) McLeish, T. C. B.; Larson, R. C. Molecular Constitutive Equations for a Class of Branched Polymers: The Pom-pom Polymer. *J. Rheol.* **1998**, *42*, 82−112.
(16) Inkson, N. J.; McLeish, T. C. B.; Harlen, O. G.; Groves, D. J. Predicting low-density polyethylene melt rheology in elongational and shear flows with the "pom-pom" constitutive equations. *J. Rheol.* **1999**, *43*, 873−896.
(17) Blackwell, R. J.; McLeish, T. C. B.; Harlen, O. G.; Molecular drag-strain coupling in polymer melts. *J. Rheol.* **2000**, *44*, 121−136.
(18) Janzen, J.; Colby, R. H. Diagnosing long-chain branching in polyethylenes. *J. Mol. Struct.* **1999**, *485−486*, 569−584.
(19) Gabriel, C.; Kokko, E.; Lofgren, B.; Seppala, J.; Münstedt, H.; Analytical and rheological characterization of long-chain branched metallocene-catalyzed ethylene homopolymers. *Polymer* **2002**, *43*, 6383−6390.
(20) Gabriel, C.; Münstedt, H. Influence of long-chain branches in polyethylenes on linear viscoelastic flow properties in shear. *Rheol. Acta* **2002**, *4*, 1232−244.
(21) Tsukahara, Y.; Namba, S.; Iwasa, N.; Kaeriyama; Takahashi, M. Bulk Properties of Poly(macromonomer)s of Increased Backbone and Branch Lengths. *Macromolecules* **2001**, *34*, 2624−2629.
(22) Kapnistos, M.; Vlassopoulos, D.; Roovers, J.; Leal, L. G. Linear rheology of architecturally complex macromolecules: Combs with linear backbones. *Macromolecules* **2005**, *38*, 8752−7862.
(23) Likhtman, A. E.; McLeish, T. C. B. Quantitative theory for linear dynamics of linear entangled polymers. *Macromolecules* **2002**, *35*, 6332−6343.
(24) Likhtman, A. E. Corrected equations for Milner-McLeish theories of stress relaxation for star and linear polymers. Unpublished note.
(25) Frischknecht, A. L.; Milner, S. T.; Pryke, A.; Young, R. N.; Hawkins, R.; McLeish, T. C. B. *Macromolecules* **2002**, *35*, 4801−4820.
(26) Larson, R. G.; Sridhar, T.; Leal, L. G.; McKinley, G. H.; Likhtman, A. E.; McLeish, T. C. B. *J. Rheol.* **2003**, *47*, 809−818.
(27) Auhl, D.; Stange, J.; Münstedt, H.; Krause, B.; Voigt, D.; Lederer, A.; Lappan, U.; Lunkwitz, K. *Macromolecules* **2004**, *37*, 9465−9472.
(28) Park, S. J.; Shanbhag, S.; Larson, R. G. *Rheol. Acta* **2005**, *44*, 319−330.
(29) Shanbhag, S.; Larson, R. G. *Macromolecules* **2004**, *37*, 8160−8166.
(30) Das, C.; Inkson, N. J.; Read, D. J.; Kelmanson, M. A.; McLeish, T. C. B. *J. Rheol.* **2006**, *50*, 207.

MA060018F